

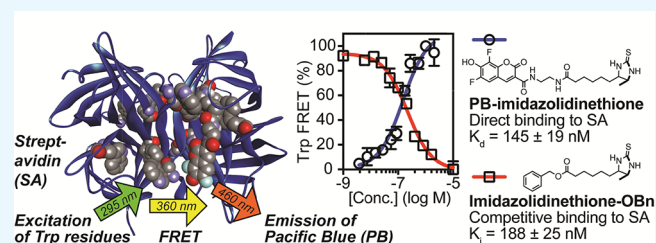
# Quantification of Small Molecule–Protein Interactions using FRET between Tryptophan and the Pacific Blue Fluorophore

Molly M. Lee and Blake R. Peterson\*<sup>✉</sup>

Department of Medicinal Chemistry, The University of Kansas, 2034 Becker Drive, Lawrence, Kansas 66047, United States

## Supporting Information

**ABSTRACT:** We report a new method to quantify the affinity of small molecules for proteins. This method is based on Förster resonance energy transfer (FRET) between endogenous tryptophan (Trp) residues and the coumarin-derived fluorophore Pacific Blue (PB). Tryptophan residues are frequently found in proteins near ligand-binding sites, making this approach potentially applicable to a wide range of systems. To improve access to PB, we developed a scalable multigram synthesis of this fluorophore, starting with inexpensive 2,3,4,5-tetrafluorobenzoic acid. This route was used to synthesize fluorescent derivatives of biotin, as well as lower affinity thiobiotin, iminobiotin, and imidazolidinethione analogues that bind the protein streptavidin. Compared with previously published FRET acceptors for tryptophan, PB proved to be superior in both sensitivity and efficiency. These unique properties of PB enabled direct quantification of dissociation constants ( $K_d$ ) as well as competitive inhibition constants ( $K_i$ ) in the micromolar to nanomolar range. In comparison to analogous binding studies using fluorescence polarization, fluorescence quenching, or fluorescence enhancement, affinities determined using Trp-FRET were more precise and accurate as validated using independent isothermal titration calorimetry studies. FRET between tryptophan and PB represents a new tool for the characterization of protein–ligand complexes.



## INTRODUCTION

To quantify the affinity of small molecules for proteins, a wide variety of biophysical techniques have been developed. Homogeneous methods include isothermal titration calorimetry (ITC),<sup>1</sup> fluorescence quenching or enhancement,<sup>2</sup> fluorescence polarization (FP),<sup>3</sup> and Förster resonance energy transfer (FRET).<sup>4</sup> Although these techniques are powerful, each has limitations. ITC, considered the gold standard for affinity determination, is material-intensive and low-throughput and requires an appreciable change in heat upon binding. In the widely employed FP (or the related fluorescence anisotropy),<sup>3,5</sup> small molecules linked to fluorophores report changes in the polarization of emitted photons when a rapidly rotating small molecule binds a slowly tumbling protein. However, probe size, solvent viscosity, fluorescence quenching, and linker flexibility can limit the applicability.<sup>3</sup>

FRET has the potential to overcome some of these limitations. This method involves nonradiative transfer of excitation (Ex.) energy from a donor fluorophore to a proximal acceptor fluorophore.<sup>4</sup> This transfer is highly distance-dependent, with an efficiency of 50% at the Förster distance ( $R_0$ , typically  $< \sim 5$  nm). FRET-based binding assays generally involve one fluorophore attached to a receptor of interest and another fluorophore conjugated to a ligand. However, this requirement for two exogenous fluorophores poses challenges, given that conjugation of fluorophores to proteins can result in heterogeneity, or requires site-directed labeling reactions.

As an alternative method for detection of small molecule–protein interactions, FRET initiated by the excitation of intrinsically fluorescent tryptophan (Trp, 1, Figure 1) residues is of increasing interest.<sup>6–8</sup> Beneficially, these residues are commonly found in or near protein–ligand binding sites and at interfaces between proteins and other biomolecules.<sup>9,10</sup> Although maximally excited at 280 nm, tryptophan can be selectively excited over tyrosine at 295 nm. Fluorescent photons emitted by tryptophan exhibit  $\lambda_{\max}$  values that range from  $\sim 308$  to  $\sim 355$  nm, roughly correlated with exposure to an aqueous solution,<sup>11</sup> typically with a modest quantum yield ( $\Phi \approx 0.2$ ). A previously reported<sup>11</sup> comparison of 19 tryptophan residues from 17 proteins with experimentally determined structures revealed an average  $\lambda_{\max}$  of tryptophan emission of 333 nm. Because the emission  $\lambda_{\max}$  and the quantum yield of tryptophan are affected by the polarity of the local environment,<sup>12</sup> its environmental sensitivity and quenching by exogenous factors have been widely used to study changes in protein conformation and binding of ligands. The intrinsic emission of tryptophan can also participate in FRET with other fluorophores,<sup>7</sup> and this approach has been extensively used to study protein folding and dynamics.<sup>13–15</sup> Fluorophores known to participate in FRET with tryptophan include derivatives of dansyl (2), 7-hydroxycoumarin (7HC, 3), and 7-dimethylami-

Received: November 2, 2016

Accepted: December 6, 2016

Published: December 19, 2016

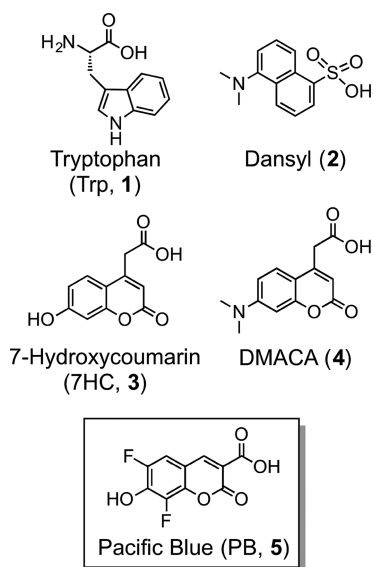


**Figure 1.** Structures of tryptophan (Trp, 1) and other fluorophores (2–5).

nocoumarin (DMACA, 4).<sup>4</sup> Coumarins 3 and 4 have recently been reported<sup>6</sup> by Chung to be the best FRET acceptors for tryptophan identified to date. However, the photophysical properties of coumarin 3 are highly sensitive to changes in pH in the physiological range (phenol  $pK_a = 7.8$ ),<sup>16,17</sup> and the absorbance<sup>18</sup> and emission<sup>19</sup> of coumarin 4 shift substantially when transitioning from an aqueous to a hydrophobic environment. Moreover, a biotin-linked derivative of coumarin 4 was reported to have a low quantum yield ( $\Phi = 0.06$ ),<sup>6</sup> which increases the concentration of the probe required for detection. These environmental effects, limited brightness, and low FRET efficiencies continue to hinder sensitivity for Trp-FRET applications. A few noncompetitive binding assays using Trp-FRET have been reported,<sup>20–23</sup> but they generally involve quenching of tryptophan fluorescence or require high concentrations of fluorescent probes for detection. These high concentrations can prevent quantitative measurements of low dissociation constants ( $K_d$ ) and competitive inhibition constants ( $K_i$ ), which are frequently observed between small molecules and proteins.

## RESULTS AND DISCUSSION

To identify a more sensitive FRET acceptor for tryptophan, we examined the overlap between the emission spectrum of this amino acid (Ex. 280 nm, Em.  $\sim 350$  nm,  $\epsilon = 5600 \text{ M}^{-1} \text{ cm}^{-1}$ ) and the absorbance spectrum of 6,8-difluoro-7-hydroxycoumarin, a fluorophore known as Pacific Blue (PB, 5).<sup>17</sup> Because of its favorable photophysical properties (Ex. 400 nm, Em. 447 nm,  $\epsilon = 29\,500 \text{ M}^{-1} \text{ cm}^{-1}$ ,  $\Phi = 0.75$ , and phenol  $pK_a = 3.7$ ), PB is of substantial interest for labeling of proteins and other biomolecules.<sup>24,25</sup> As shown in Figure 2, the large overlap between the emission of tryptophan and the absorption of PB suggested that this fluorophore might be a particularly sensitive FRET partner. To investigate this hypothesis, we developed an improved synthesis of PB that readily allows access to gram quantities of this compound (Scheme 1). In contrast to previously reported routes based on expensive 2,4-difluoro-*resorcinol*,<sup>17,26</sup> we found that the relatively inexpensive 2,3,4,5-tetrafluorobenzoic acid can be converted to the common

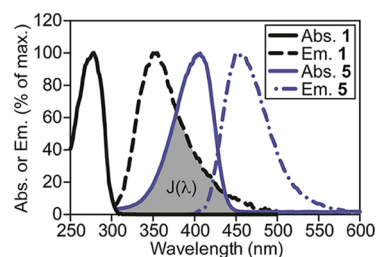
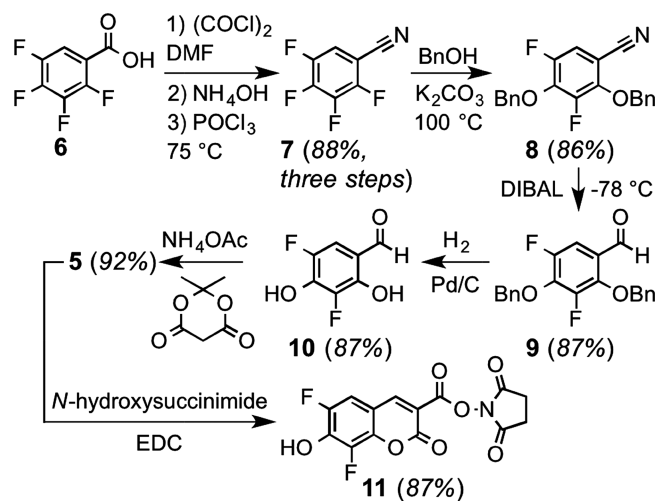


**Figure 2.** Absorbance (Abs., solid lines) and emission (Em., dotted lines) spectra of tryptophan (1, black lines, 32  $\mu\text{M}$  for Abs. and 2  $\mu\text{M}$  for Em.) and PB (5, blue lines, 32  $\mu\text{M}$  for Abs. and 50 nM for Em.) in phosphate-buffered saline (PBS, pH 7.4). The spectral overlap integral,  $J(\lambda)$ , critical for FRET, is shaded gray.

## Scheme 1. Improved Gram-Scale Synthesis of the PB Fluorophore



intermediate aldehyde **10**<sup>17,26</sup> in 66% overall yield in a four-pot process.

As a model small molecule–protein interaction, we investigated binding of the bacterial protein streptavidin (SA) to biotin and analogues. This tetrameric protein binds biotin with exceptionally high affinity ( $K_d = 10^{-14} \text{ M}^{-1}$ ),<sup>27</sup> and X-ray crystallography<sup>28</sup> has revealed six tryptophan residues in close proximity to each of its four noncooperative<sup>29</sup> biotin-binding sites. Additionally, Trp79, Trp108, and Trp120 are critical for binding of SA to biotin via van der Waals and hydrophobic interactions.<sup>28,30</sup> Moreover, in a buffered aqueous solution, excitation of these tryptophan residues leads to an average emission  $\lambda_{\text{max}}$  of 336 nm that can initiate FRET with biotinylated fluorophores.<sup>20,31,32</sup> Correspondingly, docking<sup>33</sup> of this X-ray structure (Figure 3) to PB-biotin derivative **12** (Figure 4, panel A) supported the notion that binding of SA would favorably position the fluorophore in close proximity to endogenous tryptophan residues that make noncovalent contacts to biotin and tryptophan residues in other subunits of the SA tetramer.

To compare PB (5) with known Trp-FRET acceptors (2–4), we synthesized biotin derivatives **12–15** (Figure 4, panel A). Comparison of normalized absorbance and emission spectra of these compounds (Figure 4, panel B) revealed that the PB-derived probe **12** was  $\sim 3$ -fold brighter than **14**,  $\sim 17$ -fold brighter than **15**, and more than 100-fold brighter than **13** in aqueous PBS (pH 7.4). FRET can be measured as the

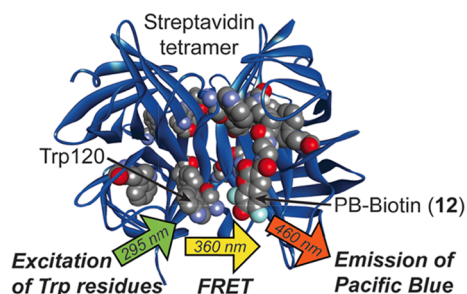


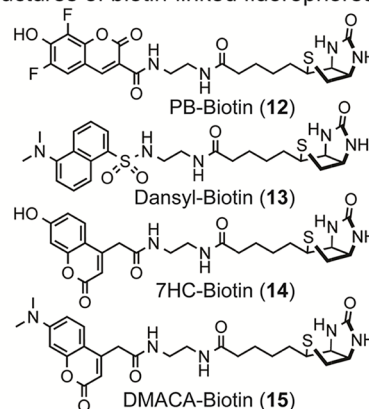
**Figure 3.** Model of SA (PDB 3RY2) docked to the PB-biotin derivative **12** (CPK model) with AutoDock Vina. In each monomer, residues Trp79, Trp108, and Trp120 are shown as CPK models. The distance between the most proximal Trp120 (marked) and the PB moiety of **12** is  $\sim 11$  Å. For clarity, only one bound ligand is shown.

relative fluorescence intensity of the donor in the absence ( $I_d$ ) and presence ( $I_{da}$ ) of the acceptor.<sup>4</sup> When probes **12–15** were added to SA, excitation of tryptophan revealed substantial differences in emission because of FRET (Figure 4, panel C). As listed in Table 1, values from these studies were used to analyze the sensitivity ( $I_{da}$ ), efficiency ( $E$ ), and other properties of these fluorophore pairs. Compared with PB (**12**), dansyl (**13**) was 33-fold less sensitive, 7HC (**14**) was 1.5-fold less sensitive, and DMACA (**15**) was 6-fold less sensitive. Additionally, the blue-shifted absorbance of 7HC (**14**) increased its excitation at 295 nm, reducing its FRET fold effect (FF) by a factor of 4. The specificity of the FRET signal of **12** upon binding to SA was confirmed by addition of biotin as a competitor (Figure 4, panel C). Consequently, PB proved to be the most efficient and sensitive FRET acceptor for tryptophan under these conditions.

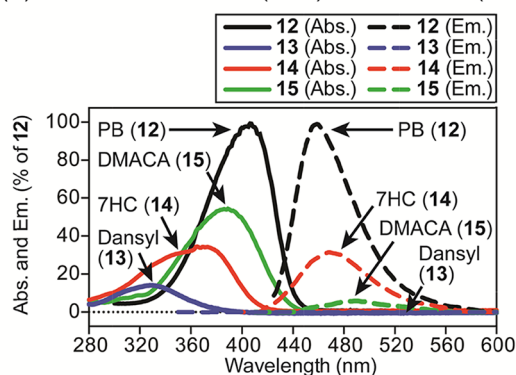
Biotin binds SA with such high affinity that its association is essentially irreversible. To investigate fluorescent analogues with lower affinity that might be suitable for equilibrium binding measurements, we synthesized probes **16–18** (Figure 5, panel A).<sup>34,35</sup> To generate equilibrium binding curves, SA was titrated into a low fixed concentration of the fluorescent probe (below  $K_d$ ), followed by excitation of tryptophan at 295 nm to trigger FRET (measured at 460 nm). Curve fitting was used to calculate the  $K_d$  values of  $11 \pm 2$  nM for thiobiotin-PB derivative **17**,  $145 \pm 19$  nM for imidazolidinethione-PB **18**, and  $2730 \pm 340$  nM for iminobiotin-PB **16** in PBS (Figure 5, panel B). These values were in excellent agreement with the independent assessments of  $K_d$  using ITC under the same conditions ( $12 \pm 4$  nM for **17** and  $125 \pm 45$  nM for **18**, Figure 5, panels C and D). For these high affinity probes, attempts to measure affinities by FP were unsuccessful because of fluorescence quenching, which affects the lifetime of the fluorophore.<sup>3</sup> However, using higher concentrations of the lower affinity probe **16**, FP yielded a comparable  $K_d$  value of  $2950 \pm 270$  nM (data shown in Supporting Information).

We hypothesized that the high sensitivity of Trp-FRET with PB might be particularly valuable for quantifying small molecule–protein interactions in a competition assay format. To test this approach, we measured competitive inhibition constants ( $K_i$ ) of the unlabeled biotin analogues **19–22** (Figure 6, panel A) using PB-imidazolidinethione **18** as a fluorescent probe. The unlabeled ligands **19–22** were added to SA (held at a concentration near the  $K_d$ ) bound to **18** (held below  $K_d$ , 25 nM). After incubation for 1 h at room temperature to achieve equilibrium, excitation of tryptophan at 295 nm was used to trigger FRET (measured at 460 nm). This approach allowed

(A) Structures of biotin-linked fluorophores



(B) Relative absorbance (Abs.) and emission (Em.)



(C) Fluor. emission upon excitation at 295 nm

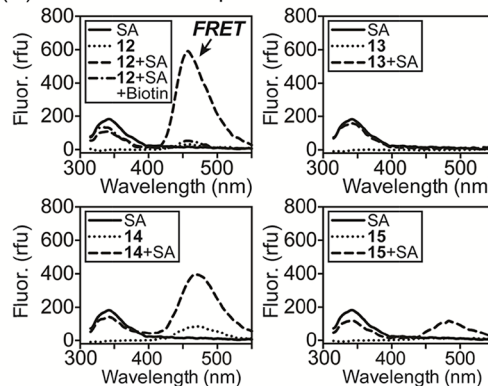


**Figure 4.** (A) Structures of fluorophores linked to biotin (**12–15**). (B) Normalized absorbance (Abs., solid lines) and fluorescence (Fluor.) emission (Em., dashed lines) spectra of **12–15** ( $32 \mu\text{M}$  for Abs.,  $50 \text{ nM}$  for Fluor.) in PBS (pH 7.4). Fluorophores **12–15** were excited at their  $\lambda_{\text{max}}$  [405 nm (**12**), 330 nm (**13**), 375 nm (**14**), and 390 nm (**15**)]. Intensities are % of  $\lambda_{\text{max}}$  of **12**. (C) Analysis of Trp-FRET upon binding of **12–15** ( $100 \text{ nM}$ ) to SA ( $[\text{monomer}] = 400 \text{ nM}$ ). Ex. of SA (295 nm) results in maximal Em. at 340 nm. After binding of **12–15**, FRET Em. was observed at 457 (**12**), 532 (**13**), 467 (**14**), and 475 nm (**15**). Addition of biotin ( $10 \mu\text{M}$ ) blocked FRET from **12**, confirming specificity.

the calculation of  $K_i$  values of  $188 \pm 25$  nM for the benzyl ester imidazolidinethione derivative **22**,  $693 \pm 91$  nM for the methyl ester imidazolidinethione **21**,  $1350 \pm 180$  nM for imidazolidinethione **20**, and  $44\,600 \pm 5800$  nM for iminobiotin **19** in PBS (Figure 6, panel B) by nonlinear curve fitting. Moreover, we independently measured the affinity of the nonfluorescent imidazolidinethione analogue **20** for SA using ITC ( $K_d = 1550 \pm 270$  nM, Figure 6, panel C), which was in excellent

**Table 1. Photophysical Properties of Fluorescent Probes<sup>a</sup>**

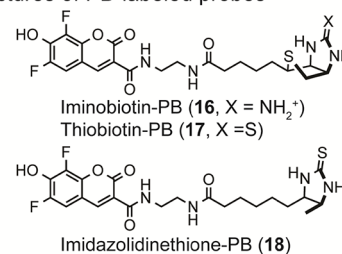
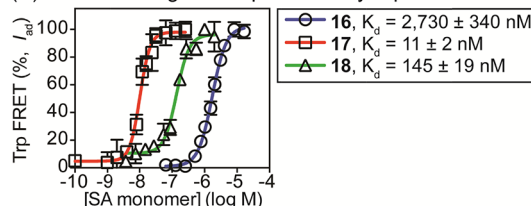
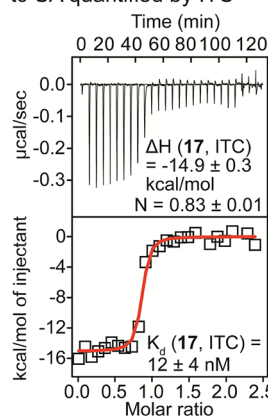
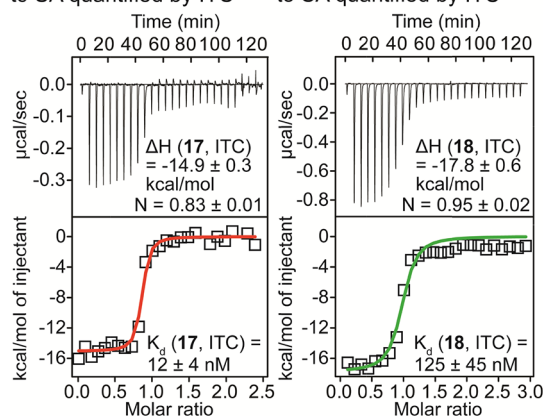
probe	$I_{ad}$	$E$	FF	$R_0$ (nm)	$\Phi_f$	$\epsilon$ ( $M^{-1}cm^{-1}$ )
12	3.3	0.40	19.2	3.0	0.74	24 200
13	0.1	0.13	6.8	2.1	0.06 <sup>8</sup>	3500
14	2.2	0.21	4.8	2.7	0.47 <sup>6</sup>	7800
15	0.6	0.35	8.0	2.8	0.06 <sup>6</sup>	11 600

<sup>a</sup>The intensity ( $I_{ad}$ ) of FRET acceptors (100 nM) was measured at Em.  $\lambda_{max}$  when bound to SA (400 nM, Ex. 295 nm) and normalized to  $I_d$ . The efficiency ( $E$ ) of FRET with tryptophan when bound to SA was calculated as  $E = 1 - I_{da}/I_d$ . FF was calculated as  $FF = I_{ad}/I_a$ .  $R_0$  is the theoretical Förster distance calculated for each Trp-acceptor pair as described in the Experimental Section.  $I_{da}$  = intensity of Em. of tryptophan (340 nm) in the presence of the acceptor.  $I_d$  = intensity of Em. of tryptophan (340 nm) in the absence of the acceptor.  $I_{ad}$  and  $I_a$  are the intensities of Em. of the acceptor [457 (12), 532 (13), 467 (14), and 475 nm (15)] in the presence and absence of the donor (SA), respectively. Values for  $\Phi_f$  and molar extinction coefficients ( $\epsilon$ ) were measured as described in the Experimental Section and Supporting Information.

agreement with the  $K_i$  quantified by Trp-FRET. Other previously published studies<sup>36,37</sup> of 19 have reported values similar to the  $K_i$  value measured by Trp-FRET.

When PB-linked ligands bind to SA, their fluorescence is partially quenched (16, 17) or enhanced (18). Hence, simple changes in fluorescence could potentially allow determination of their affinities for this protein. To examine the merits of this approach, we quantified the  $K_d$  of 16–18 for SA using only fluorescence quenching or enhancement, and we examined changes in fluorescence upon addition of the nonfluorescent competitor 20 to SA-18. As shown in Figure 7, we found that simple fluorescence quenching or enhancement could be used to estimate the affinity of 16–18 for SA, but  $K_d$  values obtained using this method differed by twofold (18) to sixfold (17) from gold-standard measurements using ITC. Moreover, examination of competitive binding of 20 to SA-18 revealed substantial deviation from the binding model at high concentrations (Figure 7, panel D), which prevented accurate determination of  $K_i$ . This lower accuracy and precision associated with the sole use of the fluorescence intensity presumably arises from its high sensitivity to aggregation of fluorophores and other environmental factors. In contrast, the dependence of FRET on the distance between fluorophores presumably reduces its susceptibility to these confounding factors. On the basis of these results, we conclude that Trp-FRET with PB is superior to fluorescence intensity measurements for quantifying equilibrium binding in this system.

In conclusion, we developed an improved synthesis of the PB fluorophore starting from inexpensive 2,3,4,5-tetrafluorobenzoic acid. This synthesis was used to prepare fluorescent molecular probes that bind the Trp-containing protein SA. Comparison with other fluorescent probes that bind SA revealed that PB is a highly sensitive and efficient FRET acceptor for tryptophan. This high sensitivity enabled quantification of  $K_d$  and competitive  $K_i$  values into the nM range. As validated using independent ITC measurements, this method proved to be more precise and accurate than analogous binding studies using fluorescence polarization, fluorescence quenching, or fluorescence enhancement for this system. FRET between tryptophan and PB offers a new method for quantification of small molecule–protein interactions.

**(A) Structures of PB-labeled probes****(B) Direct binding to SA quantified by Trp-FRET****(C) Direct binding of 17 to SA quantified by ITC****(D) Direct binding of 18 to SA quantified by ITC**

**Figure 5.** (A) Structures of analogues of biotin (16–18) used in direct binding assays. (B) Quantification of the affinity ( $K_d$ ) of SA for probes 16 (25 nM), 17 (5 nM), and 18 (25 nM) in PBS (pH 7.4) by Trp-FRET. Tryptophan residues were excited at 295 nm and FRET was measured at 460 nm. Values were corrected to account for fluorescence quenching or enhancement upon binding, as described in Experimental Section. [SA] was based on monomeric protein. Dissociation constants ( $K_d$ ) were calculated using a one-site binding model (GraphPad Prism 6.0). (C,D) Quantification of the binding of 17 (C) and 18 (D) to SA in PBS (pH 7.4) using ITC. Thermodynamic parameters and  $K_d$  values were calculated with Origin software. For 17, [SA in sample cell] = 4  $\mu$ M and [17 in syringe] = 50  $\mu$ M. For 18, [SA in sample cell] = 10  $\mu$ M and [18 in syringe] = 150  $\mu$ M.

## EXPERIMENTAL SECTION

**Synthesis.** Chemicals were purchased from Sigma Aldrich, Acros Organics, Alfa Aesar, Oakwood Chemical, or Chem-Impex International. All nonaqueous reactions were carried out using flame- or oven-dried glassware under an atmosphere of dry argon or nitrogen. Tetrahydrofuran (THF), dichloromethane ( $CH_2Cl_2$ ), *N,N*-dimethylformamide (DMF), and methanol ( $CH_3OH$ ) were purified via filtration through two columns of activated basic alumina under an atmosphere of Ar using a solvent purification system from Pure Process Technology (GlassContour). Other commercial reagents were used as received unless otherwise noted. <sup>1</sup>H nuclear magnetic resonance (NMR), <sup>13</sup>C NMR, and <sup>19</sup>F NMR spectra were acquired on a Bruker DRX-400 or an Avance AVIII 500 MHz

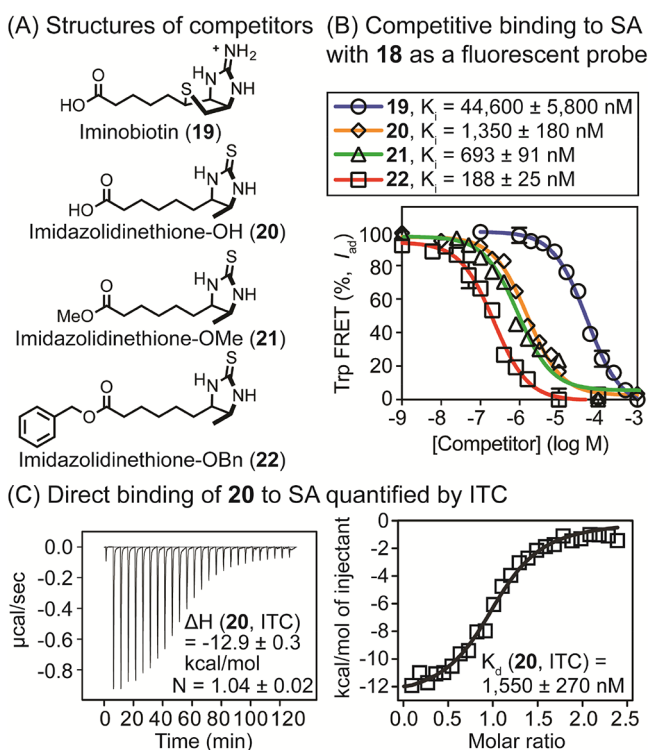


**Figure 6.** (A) Structures of nonfluorescent analogues of biotin (19–22) used in competition binding assays. (B) Quantification of competitive inhibitory constants ( $K_i$ ) of 19–22 for SA complexed with 18 (175 nM for SA and 25 nM for 18) by Trp-FRET. Tryptophan residues were excited at 295 nm, and FRET was measured at 460 nm. Values were corrected to account for fluorescence quenching upon binding as described in Experimental Section. [SA] was based on monomeric protein. Half-maximal inhibitory concentrations ( $IC_{50}$ ) were calculated using a log(inhibitor) vs response model (GraphPad Prism 6.0), and  $IC_{50}$  values were converted to  $K_i$  values. (C) Evaluation of direct binding of 20 to SA using ITC. Compound 20 was titrated into [SA] in PBS (pH 7.4), and thermodynamic parameters and  $K_d$  values were calculated using the Origin software. [SA in sample cell] = 20  $\mu$ M and [20 in syringe] = 250  $\mu$ M.

instrument. For  $^1\text{H}$  and  $^{13}\text{C}$ , chemical shifts ( $\delta$ ) are reported in ppm referenced to  $\text{CDCl}_3$  (7.26 ppm for  $^1\text{H}$  and 77.2 ppm for  $^{13}\text{C}$ ),  $\text{CD}_3\text{OD}$  (3.31 ppm for  $^1\text{H}$ , 49.0 ppm for  $^{13}\text{C}$ ), or dimethyl sulfoxide ( $\text{DMSO}-d_6$ ) (2.50 ppm for  $^1\text{H}$ , 39.5 ppm for  $^{13}\text{C}$ ). For  $^{19}\text{F}$ , chemical shifts ( $\delta$ ) are reported in ppm referenced to trifluoroethanol ( $-77.0$  ppm for  $^{19}\text{F}$ ).  $^1\text{H}$  coupling constants ( $J_{\text{HH}}$ , Hz),  $^{13}\text{C}$  coupling constants ( $J_{\text{CF}}$ , Hz), and  $^{19}\text{F}$  coupling constants ( $J_{\text{FF}}$ , Hz) are reported as chemical shift, multiplicity (br = broad, s = singlet, d = doublet, t = triplet, q = quartet, and m = multiplet), coupling constant, and integration. High-resolution mass spectra were obtained at the Mass Spectrometry Laboratory at the University of Kansas on a Micromass LCT Premier. Thin layer chromatography (TLC) was performed using EMD aluminum-backed (0.20 mm) silica plates (60 F-254), and flash chromatography used ICN silica gel (200–400 mesh). TLC plates were visualized with a UV lamp or by staining with  $\text{I}_2$ . Preparative high-performance liquid chromatography (HPLC) was performed with an Agilent 1200 instrument equipped with a Hamilton PRP-1 reverse phase column (250 mm length, 21.2 mm ID, and 7  $\mu$ m particle size) with detection by absorbance at 215, 254, and 370 nm.

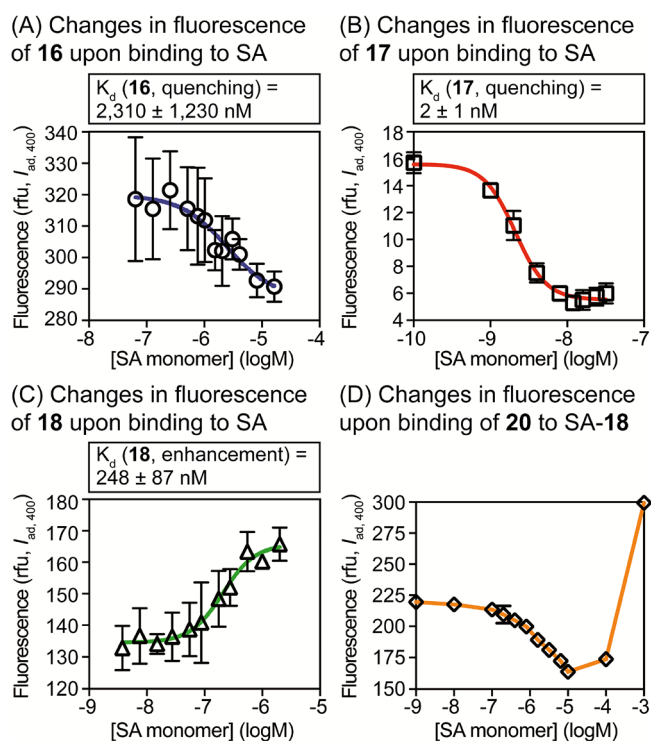


**Figure 7.** Analysis of interactions with SA by quenching or enhancement of fluorescence. PB was excited at 400 nm, and the intensity of fluorescence emission at 460 nm was measured. (A–C) Quantification of  $K_d$  values for direct binding. (D) Fluorescence resulting from competition of 20 for SA bound to probe 18 (25 nM). In (D), because of the poor fit to the binding model, the  $K_i$  value was not calculated.

**2,3,4,5-Tetrafluorobenzonitrile (7).** To a solution of 2,3,4,5-tetrafluorobenzoic acid (6, 10 g, 51 mmol) in  $\text{CH}_2\text{Cl}_2$  (50 mL) was added oxalyl chloride (5.4 mL, 62.9 mmol) and DMF (ca. 2 drops), and the reaction mixture was stirred at 22  $^\circ\text{C}$  for 16 h while venting to the atmosphere to allow escape of evolved gases. The solvent was removed under reduced pressure, and the vessel was placed on high vacuum for 2 h to afford the acid chloride as a viscous oil. This oil was dissolved in chloroform (40 mL) and cooled to 4  $^\circ\text{C}$ . Aqueous ammonia (28%, 55 mL) was slowly added and the reaction was stirred at 4  $^\circ\text{C}$  for 30 min. The mixture was extracted with chloroform, and the organic layer was dried, filtered, and concentrated under reduced pressure to afford a white solid. To this solid was added phosphoryl chloride (32 mL), and the mixture was stirred at 80  $^\circ\text{C}$  for 3 h. This mixture was treated with diethyl ether (150 mL) and ice water (100 mL), followed by sat. aqueous  $\text{NaHCO}_3$  (100 mL) for 1 h. This mixture was extracted with diethyl ether, and the organic layer was washed with sat. aqueous  $\text{NaHCO}_3$  ( $3 \times 100$  mL). The organic layer was dried, filtered, and concentrated under reduced pressure to afford 7 (7.9 g, 88%) as a colorless oil.  $^1\text{H}$  NMR (500 MHz,  $\text{CDCl}_3$ )  $\delta$  7.33 (dddd,  $J = 8.8, 7.6, 5.3, 2.6$  Hz, 1H);  $^{13}\text{C}$  NMR (126 MHz,  $\text{CDCl}_3$ )  $\delta$  149.5 (dddd,  $J = 269.0, 12.1, 4.0, 2.0$  Hz), 147.4 (dddd,  $J = 259.0, 10.8, 3.9, 2.2$  Hz), 144.4 (dddd,  $J = 265.6, 15.9, 12.2, 3.2$  Hz), 143.4 (ddd,  $J = 16.0, 12.1, 3.2$  Hz), 141.3 (dddd,  $J = 258.6, 15.0, 12.7, 4.0$  Hz), 115.0 (dd,  $J = 21.9, 4.1$  Hz), 111.2 (m), 97.8 (dddd,  $J = 14.2, 9.3, 4.7, 1.7$  Hz);  $^{19}\text{F}$  NMR (376 MHz,  $\text{CDCl}_3$ )  $\delta$   $-129.99$  (dddt,  $J = 31.8, 19.9, 11.9, 6.9$  Hz),  $-134.49$  (dddt,  $J = 32.4, 20.6, 11.8, 5.3$  Hz),  $-143.33$  (tdd,  $J = 20.5, 12.9, 8.3$  Hz),  $-150.62$  (dddd,  $J = 39.3, 24.4,$

17.3, 6.4 Hz); HRMS (ESI<sup>-</sup>)  $m/z$  173.9993 ( $M - H^+$ ,  $C_7F_4N$  requires 173.9967). Note that this compound is commercially available (e.g. Alfa Aesar, 25 g/\$173).

**2,4-Bis(benzyloxy)-3,5-difluorobenzonitrile (8).** To a solution of **7** (7.8 g, 45 mmol) in DMF (5 mL) was added benzyl alcohol (23 mL, 223 mmol) and potassium carbonate (37 g, 267 mmol). The vessel was heated to 105 °C for 16 h, subsequently placed under high vacuum for 2 h to remove DMF, followed by purification using column chromatography on silica gel (eluent: hexanes/ethyl acetate (17:1)) to afford **8** (13.5 g, 86%) as a viscous colorless oil. <sup>1</sup>H NMR (500 MHz, CDCl<sub>3</sub>) δ 7.46–7.33 (m, 11H), 7.04 (dd,  $J = 10.0, 2.3$  Hz, 1H), 5.29 (s, 2H), 5.2251 (d,  $J = 1.0$  Hz, 2H); <sup>13</sup>C NMR (126 MHz, CDCl<sub>3</sub>) δ 151.1 (dd,  $J = 247.5, 4.8$  Hz), 149.4 (dd,  $J = 251.5, 6.3$  Hz), 146.3 (dd,  $J = 11.9, 3.3$  Hz), 140.7 (dd,  $J = 14.7, 12.1$  Hz), 135.5, 135.2, 129.1, 129.0, 128.84, 128.80, 128.77, 128.4, 114.9 (dd,  $J = 23.6, 3.7$  Hz), 114.8 (d,  $J = 3.0$  Hz), 101.0 (dd,  $J = 10.5, 5.0$  Hz), 76.8 (d,  $J = 5.6$  Hz), 76.2 (t,  $J = 3.9$  Hz); <sup>19</sup>F NMR (376 MHz, CDCl<sub>3</sub>) δ -129.79 (d,  $J = 6.9$  Hz), -138.96 (d,  $J = 6.9$  Hz); HRMS (ESI<sup>+</sup>)  $m/z$  374.0979 ( $M + Na^+$ ,  $C_{21}H_{15}F_2NO_2Na$  requires 374.0969).

**2,4-Bis(benzyloxy)-3,5-difluorobenzaldehyde (9).** To a solution of **8** (13.4 g, 38 mmol) in CH<sub>2</sub>Cl<sub>2</sub> (20 mL) at -78 °C was added diisobutylaluminum hydride (Acros Organics, 1 M in cyclohexane, 45.9 mL). The reaction mixture was stirred at -78 °C for 3.5 h and was then warmed to 22 °C. The reaction was quenched with aqueous HCl (0.5 M, 150 mL) by stirring for 1 h. The mixture was extracted with ethyl acetate, dried, filtered, and evaporated under reduced pressure. The resultant solid was recrystallized from ethanol to afford **9** (11.6 g, 87%) as a white solid. <sup>1</sup>H NMR (500 MHz, CDCl<sub>3</sub>) δ 10.01 (d,  $J = 3.3$  Hz, 1H), 7.49–7.27 (m, 11H), 5.34 (s, 2H), 5.17 (d,  $J = 1.0$  Hz, 2H); <sup>13</sup>C NMR (126 MHz, CDCl<sub>3</sub>) δ 187.1 (dd,  $J = 3.2, 1.8$  Hz), 151.8 (dd,  $J = 247.3, 4.0$  Hz), 149.1 (dd,  $J = 250.8, 5.5$  Hz), 146.6 (dd,  $J = 10.1, 2.9$  Hz), 141.6 (dd,  $J = 15.4, 12.2$  Hz), 135.8, 135.3, 129.2, 128.94, 128.91, 128.90, 128.8, 128.4, 124.1 (dd,  $J = 6.3, 1.6$  Hz), 109.2 (dd,  $J = 21.2, 3.1$  Hz), 77.4 (d,  $J = 6.5$  Hz), 76.0 (t,  $J = 4.0$  Hz); <sup>19</sup>F NMR (376 MHz, CDCl<sub>3</sub>) δ -130.48 (d,  $J = 5.7$  Hz), -140.71 (dd,  $J = 6.0, 2.5$  Hz); HRMS (ESI<sup>+</sup>)  $m/z$  377.0983 ( $M + Na^+$ ,  $C_{21}H_{16}F_2O_3Na$  requires 377.0965).

**3,5-Difluoro-2,4-dihydroxybenzaldehyde (10).** To a solution of **9** (11.0 g, 31 mmol) in CH<sub>3</sub>OH/THF (100 mL, 7:3) was added Pd/C (10%, 1.67 g), and the mixture was stirred under an atmosphere of hydrogen (1 atm) at 22 °C for 8 h. After removing the catalyst by filtration over celite, the filtrate was concentrated under reduced pressure and purified using column chromatography over silica gel (eluent: hexanes/ethyl acetate/acetic acid (82:18:1)) to afford **10** (4.6 g, 83%) as a light pink solid. <sup>1</sup>H NMR (500 MHz, DMSO-*d*<sub>6</sub>) δ 11.58 (s, 1H), 10.86 (s, 1H), 10.0439 (d,  $J = 2.4$  Hz, 1H), 7.29 (dd,  $J = 10.8, 2.1$  Hz, 1H); <sup>13</sup>C NMR (126 MHz, DMSO-*d*<sub>6</sub>) δ 189.5, 146.8 (d,  $J = 11.8$  Hz), 145.6 (dd,  $J = 236.6, 4.5$  Hz), 141.5 (dd,  $J = 18.0, 13.5$  Hz), 141.2 (dd,  $J = 238.9, 5.7$  Hz), 113.9 (d,  $J = 5.8$  Hz), 109.4 (dd,  $J = 19.4, 2.9$  Hz); <sup>19</sup>F NMR (376 MHz, DMSO-*d*<sub>6</sub>) δ -144.25, -156.25 (d,  $J = 6.4$  Hz); HRMS (ESI<sup>-</sup>)  $m/z$  173.0038 ( $M - H^+$ ,  $C_7H_3F_2O_3$  requires 173.0050). Note: This product can be carried forward without further purification. Following simple filtration through celite and concentration, this crude material has yielded PB (**5**) in high purity (79% yield over two steps, 8.5 mmol scale).

**6,8-Difluoro-7-hydroxy-2-oxo-2H-chromene-3-carboxylic Acid (PB, 5).** To a suspension of **10** (4.2 g, 24.1 mmol) in water

(110 mL) was added Meldrum's acid (3.8 g, 26.6 mmol) and ammonium acetate (550 mg, 7.2 mmol). The suspension was stirred at 22 °C for 3.5 h. Aqueous HCl (2 M, 75 mL) was added, and the mixture was placed at 4 °C for 1 h. A precipitate that formed was filtered, washed with cold water (2 × 25 mL), and dried under high vacuum to afford PB (**5**, 5.4 g, 92%) as a light yellow solid. <sup>1</sup>H NMR (500 MHz, DMSO-*d*<sub>6</sub>) δ 8.67 (d,  $J = 1.4$  Hz, 1H), 7.66 (dd,  $J = 10.5, 2.0$  Hz, 1H); <sup>13</sup>C NMR (126 MHz, DMSO-*d*<sub>6</sub>) δ 163.9, 155.6, 148.6 (dd,  $J = 240.8, 4.7$  Hz), 148.5 (t,  $J = 2.9$  Hz), 141.3 (d,  $J = 9.6$  Hz), 140.3 (dd,  $J = 18.1, 12.6$  Hz), 138.7 (dd,  $J = 244.7, 6.4$  Hz), 115.3, 110.5 (dd,  $J = 20.9, 3.0$  Hz), 109.0 (d,  $J = 10.2$  Hz). <sup>19</sup>F NMR (376 MHz, DMSO-*d*<sub>6</sub>) δ -137.33 (d,  $J = 9.3$  Hz), -155.68 (d,  $J = 9.8$  Hz); HRMS (ESI<sup>-</sup>)  $m/z$  240.9944 ( $M - H^+$ ,  $C_{10}H_3F_2O_5$  requires 240.9949).

**2,5-Dioxopyrrolidin-1-yl 6,8-Difluoro-7-hydroxy-2-oxo-2H-chromene-3-carboxylate (PB NHS Ester, 11).** To a solution of **5** (0.75 g, 3.1 mmol) in DMF (5 mL) was added *N*-(3-dimethylaminopropyl)-*N'*-ethylcarbodiimide hydrochloride (EDC, 1.2 g, 6.2 mmol) and *N*-hydroxysuccinimide (0.89 g, 7.8 mmol). This mixture was stirred at 22 °C for 16 h and was subsequently added dropwise to cold aq HCl (1 N, 75 mL). A precipitate formed, which was filtered, washed with cold aq HCl (1 N, 25 mL), and dried under high vacuum to give **11** (920 mg, 87%) as a yellow solid. <sup>1</sup>H NMR (500 MHz, DMSO-*d*<sub>6</sub>) δ 9.01 (d,  $J = 1.4$  Hz, 1H), 7.78 (dd,  $J = 10.2, 1.9$  Hz, 1H), 2.89 (s, 4H); <sup>13</sup>C NMR (126 MHz, DMSO-*d*<sub>6</sub>) δ 170.3, 158.4, 154.4, 152.1 (t,  $J = 2.9$  Hz), 148.8 (dd,  $J = 241.3, 4.9$  Hz), 142.4 (d,  $J = 9.0$  Hz), 138.7 (dd,  $J = 244.8, 6.6$  Hz), 111.5 (dd,  $J = 21.1, 2.8$  Hz), 108.8, 108.4 (d,  $J = 10.3$  Hz), 25.6; <sup>19</sup>F NMR (376 MHz, DMSO-*d*<sub>6</sub>) δ -136.84, -155.95 (d,  $J = 13.4$  Hz); HRMS (ESI<sup>-</sup>)  $m/z$  338.0129 ( $M - H^+$ ,  $C_{14}H_6F_2NO_7$  requires 338.0112).

**General Procedure for the Synthesis of Fluorescent Derivatives of Biotin. General Procedure A (12, 13).** *N*-Boc-ethylenediamine-*D*-biotin (64–87 mg, 1.5 equiv), prepared as previously reported,<sup>38</sup> was treated with a solution of trifluoroacetic acid (TFA) in CH<sub>2</sub>Cl<sub>2</sub> (2 mL, 30:70) for 20 min. The mixture was concentrated under vacuum and washed with CH<sub>2</sub>Cl<sub>2</sub> (5 mL) and diethyl ether (5 mL × 2) to remove excess TFA. The activated fluorophore (1 equiv), *N,N*-diisopropylethylamine (DIEA, 5 equiv), and DMF (1–3 mL) were added, and the reaction mixture was stirred at 22 °C for 16 h. The solvent was removed under vacuum, the residue was dissolved in DMSO (1.5 mL), and the product was purified by preparative reversed-phase (RP)-HPLC [gradient: H<sub>2</sub>O:CH<sub>3</sub>CN (9:1) to (0:100) with added TFA (0.1%) over 20 min; elution time = 6–10 min]. Pure fractions were collected and combined, and the solvent was removed using lyophilization.

**General Procedure B (14, 15).** *N*-Boc-ethylenediamine-*D*-biotin (92–120 mg, 1.5 equiv), prepared as previously reported,<sup>38</sup> was treated with a solution of TFA/CH<sub>2</sub>Cl<sub>2</sub> (2 mL, 30:70) for 20 min. The mixture was concentrated under vacuum and washed with CH<sub>2</sub>Cl<sub>2</sub> (5 mL) and ether (5 mL × 2) to remove excess TFA. The fluorophore (1 equiv), 1-ethyl-3-(3-dimethylaminopropyl)carbodiimide (EDC, 1.1 equiv), 4-dimethylaminopyridine (DMAP, 0.5 equiv), and DMF (2 mL) were added, and the reaction mixture was stirred at 22 °C for 16 h. The solvent was removed under vacuum, the residue was dissolved in DMSO (1.5 mL), and the product was purified by preparative RP-HPLC (gradient: H<sub>2</sub>O:CH<sub>3</sub>CN (9:1) to (0:100) with added TFA (0.1%) over 20 min; elution time =

6–10 min). Pure fractions were collected, combined, and dried using lyophilization.

**6,8-Difluoro-7-hydroxy-2-oxo-N-(2-(5-((3aS,4S,6aR)-2-oxohexahydro-1H-thieno[3,4-d]imidazol-4-yl)pentanamido)ethyl)-2H-chromene-3-carboxamide (PB-Biotin, 12).** Following the general procedure A, PB NHS ester (**11**, 50 mg, 0.15 mmol) yielded compound **12** (45 mg, 60%) as a pale yellow solid.  $^1\text{H}$  NMR (500 MHz, DMSO- $d_6$ )  $\delta$  8.82 (d,  $J$  = 1.4 Hz, 1H), 8.67 (t,  $J$  = 5.8 Hz, 1H), 7.93 (t,  $J$  = 5.6 Hz, 1H), 7.78 (dd,  $J$  = 10.5, 1.9 Hz, 1H), 6.44 (s, 1H), 6.36 (s, 1H), 4.29 (dd,  $J$  = 7.7, 4.9 Hz, 1H), 4.11 (dd,  $J$  = 7.8, 4.4 Hz, 1H), 3.39 (q,  $J$  = 6.2 Hz, 2H), 3.22 (q,  $J$  = 6.1 Hz, 2H), 3.07 (ddd,  $J$  = 8.5, 6.3, 4.4 Hz, 1H), 2.78 (dd,  $J$  = 12.4, 5.1 Hz, 1H), 2.55 (d,  $J$  = 12.4 Hz, 1H), 2.06 (t,  $J$  = 7.4 Hz, 2H), 1.64–1.26 (m, 6H);  $^{13}\text{C}$  NMR (126 MHz, DMSO- $d_6$ )  $\delta$  172.3, 162.7, 161.3, 159.5, 148.8 (dd,  $J$  = 241.2, 4.6 Hz), 147.3 (t,  $J$  = 2.9 Hz), 140.5 (d,  $J$  = 9.2 Hz), 140.0 (d,  $J$  = 13.2 Hz), 138.8 (dd,  $J$  = 245.1, 6.6 Hz), 116.2, 110.6 (dd,  $J$  = 21.0, 3.0 Hz), 109.6 (d,  $J$  = 10.2 Hz), 61.0, 59.2, 55.4, 40.1, 39.4, 38.5, 38.1, 35.2, 28.2, 28.1, 28.0, 25.3; HRMS (ESI $^-$ )  $m/z$  509.1298 ( $M - \text{H}^+$ ,  $\text{C}_{22}\text{H}_{23}\text{F}_2\text{N}_4\text{O}_6\text{S}$  requires 509.1306).

**N-(2-(5-(Dimethylamino)naphthalene)-1-sulfonamido)ethyl)-5-((3aS,4S,6aR)-2-oxohexahydro-1H-thieno[3,4-d]imidazol-4-yl)pentanamide (Dansyl-Biotin, 13).** Following the general procedure A, dansyl chloride (30 mg, 0.11 mmol) yielded compound **13** (25 mg, 42%) as a white solid.  $^1\text{H}$  NMR (500 MHz, DMSO- $d_6$ )  $\delta$  8.47 (dt,  $J$  = 8.6, 1.1 Hz, 1H), 8.28 (dt,  $J$  = 8.8, 0.9 Hz, 1H), 8.10 (dd,  $J$  = 7.3, 1.2 Hz, 1H), 7.99 (t,  $J$  = 5.9 Hz, 1H), 7.73 (t,  $J$  = 5.8 Hz, 1H), 7.62 (m, 2H), 7.28 (d,  $J$  = 7.4 Hz, 1H), 6.42 (s, 1H), 4.30 (dd,  $J$  = 7.4, 4.7 Hz, 1H), 4.11 (dd,  $J$  = 7.7, 4.4 Hz, 1H), 3.13–3.05 (m, 1H), 3.03 (dt,  $J$  = 7.5, 5.9 Hz, 2H), 2.85 (s, 6H), 2.83–2.75 (m, 3H), 2.57 (d,  $J$  = 12.5 Hz, 1H), 1.93 (t,  $J$  = 7.4 Hz, 2H), 1.66–1.15 (m, 6H).  $^{13}\text{C}$  NMR (126 MHz, DMSO- $d_6$ )  $\delta$  172.2, 162.7, 158.3, 158.0, 151.2, 135.8, 129.5, 129.0, 128.4, 128.3, 127.9, 123.7, 117.0, 115.2, 114.7, 61.0, 59.2, 55.4, 45.1, 42.0, 39.5, 35.1, 28.2, 25.1; HRMS (ESI $^+$ )  $m/z$  542.1900 ( $M + \text{Na}^+$ ,  $\text{C}_{24}\text{H}_{33}\text{N}_5\text{O}_4\text{S}_2\text{Na}$  requires 542.1872).

**N-(2-(2-(7-Hydroxy-2-oxo-2H-chromen-4-yl)acetamido)ethyl)-5-((3aS,4S,6aR)-2-oxohexahydro-1H-thieno[3,4-d]imidazol-4-yl)pentanamide (7-Hydroxycoumarin-Biotin, 7HC-Biotin, 14).** 2-(7-Hydroxy-2-oxo-2H-chromen-4-yl)acetic acid was prepared as previously reported.<sup>39</sup> Following the general procedure B, 2-(7-hydroxy-2-oxo-2H-chromen-4-yl)acetic acid (45 mg, 0.21 mmol) yielded compound **14** (57 mg, 57%) as a yellow solid.  $^1\text{H}$  NMR (500 MHz, DMSO- $d_6$ )  $\delta$  10.57 (s, 1H), 8.27–8.15 (m, 1H), 7.93–7.75 (m, 1H), 7.58 (d,  $J$  = 8.7 Hz, 1H), 6.79 (dd,  $J$  = 8.7, 2.4 Hz, 1H), 6.71 (d,  $J$  = 2.4 Hz, 1H), 6.40 (d,  $J$  = 27.8 Hz, 2H), 6.16 (s, 1H), 4.30 (dd,  $J$  = 7.7, 5.0 Hz, 1H), 4.12 (ddd,  $J$  = 7.7, 4.4, 1.8 Hz, 1H), 3.74–3.50 (m, 2H), 3.09 (m, 5H), 2.81 (dd,  $J$  = 12.4, 5.1 Hz, 1H), 2.57 (d,  $J$  = 12.5 Hz, 2H), 2.02 (t,  $J$  = 7.4 Hz, 2H), 1.67–1.18 (m, 6H);  $^{13}\text{C}$  NMR (126 MHz, DMSO)  $\delta$  172.3, 167.8, 162.7, 161.2, 160.3, 155.0, 151.1, 126.8, 112.9, 111.9, 111.5, 102.3, 61.0, 59.2, 55.4, 40.4, 40.1, 40.0, 39.94, 39.86, 39.78, 39.69, 39.61, 39.5, 39.4, 39.2, 39.0, 38.9, 38.7, 38.1, 35.2, 28.2, 28.1, 25.2; HRMS (ESI $^-$ )  $m/z$  487.1647 ( $M - \text{H}^+$ ,  $\text{C}_{23}\text{H}_{27}\text{N}_4\text{O}_6\text{S}$  requires 487.1651).

**N-(2-(2-(7-(Dimethylamino)-2-oxo-2H-chromen-4-yl)acetamido)ethyl)-5-((3aS,4S,6aR)-2-oxohexahydro-1H-thieno[3,4-d]imidazol-4-yl)pentanamide (DMACA-Biotin, 15).** 2-(7-(Dimethylamino)-2-oxo-2H-chromen-4-yl)acetic acid was prepared as previously reported.<sup>39</sup> Following the

general procedure B, 2-(7-(dimethylamino)-2-oxo-2H-chromen-4-yl)acetic acid (DMACA, 40 mg, 0.16 mmol) yielded compound **15** (36 mg, 43%) as a yellow solid.  $^1\text{H}$  NMR (500 MHz, DMSO- $d_6$ )  $\delta$  8.25–8.18 (m, 1H), 7.82 (d,  $J$  = 5.4 Hz, 1H), 7.53 (d,  $J$  = 9.0 Hz, 1H), 6.73 (dd,  $J$  = 9.0, 2.6 Hz, 1H), 6.56 (d,  $J$  = 2.5 Hz, 1H), 6.46–6.41 (m, 1H), 6.38 (s, 1H), 6.00 (s, 1H), 4.30 (ddd,  $J$  = 7.7, 5.2, 1.0 Hz, 1H), 4.16–4.10 (m, 1H), 3.61–3.57 (m, 2H), 3.10 (m, 5H), 3.02 (s, 6H), 2.82 (dd,  $J$  = 12.4, 5.1 Hz, 1H), 2.58 (d,  $J$  = 12.5 Hz, 1H), 2.03 (t,  $J$  = 7.4 Hz, 2H), 1.69–1.18 (m, 6H);  $^{13}\text{C}$  NMR (126 MHz, DMSO)  $\delta$  172.7, 168.4, 163.2, 161.2, 155.8, 153.2, 151.6, 126.5, 109.9, 109.5, 108.7, 97.9, 61.5, 59.6, 55.9, 40.9, 39.3, 39.1, 38.6, 35.7, 28.7, 28.5, 25.6; HRMS (ESI $^+$ )  $m/z$  516.2291 ( $M + \text{H}^+$ ,  $\text{C}_{25}\text{H}_{34}\text{N}_5\text{O}_5\text{S}$  requires 516.2281).

**tert-Butyl(2-(6,8-difluoro-7-hydroxy-2-oxo-2H-chromene-3-carboxamido)ethyl)carbamate (N-Boc-ethylenediamine-PB, 23).** To a solution of **11** (200 mg, 0.59 mmol) in DMF (5 mL) was added *N*-Boc-ethylenediamine (114 mg, 0.71 mmol). The reaction mixture was stirred at 22 °C for 16 h. The vessel was placed under high vacuum for 1 h to remove DMF (4 mL). The remaining reaction mixture was added dropwise to cold aq HCl (1 N, 40 mL). A precipitate formed, which was filtered, washed with cold aq HCl (1 N, 10 mL), and dried under high vacuum to give **23** (200 mg, 88%) as a yellow solid.  $^1\text{H}$  NMR (500 MHz, DMSO- $d_6$ )  $\delta$  8.81 (d,  $J$  = 1.4 Hz, 1H), 8.67 (t,  $J$  = 5.8 Hz, 1H), 7.77 (dd,  $J$  = 10.4, 1.9 Hz, 1H), 6.95 (t,  $J$  = 5.6 Hz, 1H), 3.36 (q,  $J$  = 6.1 Hz, 2H), 3.10 (q,  $J$  = 6.0 Hz, 2H), 1.37 (s, 11H), 1.45–1.39 (m, 1H);  $^{13}\text{C}$  NMR (126 MHz, DMSO- $d_6$ )  $\delta$  161.3, 159.5, 155.7, 148.9 (dd,  $J$  = 240.9, 4.8 Hz), 147.3, 140.5 (d,  $J$  = 9.0 Hz), 140.1, 138.8 (dd,  $J$  = 245.0, 6.4 Hz), 116.2, 110.7, 110.5, 109.5, 109.5, 77.7, 28.2; HRMS (ESI $^-$ )  $m/z$  383.1043 ( $M - \text{H}^+$ ,  $\text{C}_{17}\text{H}_{17}\text{F}_2\text{N}_2\text{O}_6$  requires 383.1055).

**General Procedure for the Synthesis of Analogues of Biotin Linked to PB. General Procedure C (16–18).** *N*-Boc-ethylenediamine-PB (**23**, 23–29 mg, 1 equiv) was treated with a solution of TFA in  $\text{CH}_2\text{Cl}_2$  (2 mL, 30:70) for 20 min. The mixture was concentrated and washed with  $\text{CH}_2\text{Cl}_2$  (5 mL) and MeOH (5 mL  $\times$  2) to remove excess TFA. The biotin analogue (1.3 equiv), HBTU (1.5 equiv), hydroxybenzotriazole (HOBt, 1.5 equiv), DIEA (5 equiv), and DMF (1 mL) were added. The reaction mixture was stirred at 22 °C for 16 h. The solvent was removed under vacuum, the residue was dissolved in DMSO (1.5 mL), and the product was purified by preparative RP-HPLC (gradient:  $\text{H}_2\text{O}:\text{CH}_3\text{CN}$  (9:1) to (0:100) with added TFA (0.1%) over 20 min; elution time = 6–10 min). Pure fractions were collected, combined, and dried using lyophilization.

**(3aS,4S,6aR)-4-(5-((2-(6,8-Difluoro-7-hydroxy-2-oxo-2H-chromene-3-carboxamido)ethyl)amino)-5-oxopentyl)-tetrahydro-1H-thieno[3,4-d]imidazol-2(3H)-iminium (PB-Iminobiotin, 16).** Following the general procedure C, 2-iminobiotin (19 mg, 0.077 mmol) yielded compound **16** (12 mg, 40%) as a pale yellow solid.  $^1\text{H}$  NMR (500 MHz, DMSO- $d_6$ )  $\delta$  8.80 (d,  $J$  = 1.4 Hz, 1H), 8.67 (t,  $J$  = 5.8 Hz, 1H), 8.22 (d,  $J$  = 6.5 Hz, 1H), 8.11–8.01 (m, 1H), 7.94 (t,  $J$  = 5.6 Hz, 1H), 7.82–7.70 (m, 1H), 7.62 (s, 2H), 6.55 (s, 1H), 4.63 (dd,  $J$  = 7.9, 4.8 Hz, 1H), 4.44 (ddd,  $J$  = 7.9, 4.5, 1.7 Hz, 1H), 3.38 (d,  $J$  = 6.3 Hz, 2H), 3.22 (dd,  $J$  = 7.7, 3.7 Hz, 2H), 3.01–2.82 (m, 2H), 2.77 (d,  $J$  = 12.9 Hz, 1H), 2.07 (t,  $J$  = 7.3 Hz, 2H), 1.75–1.23 (m, 6H);  $^{13}\text{C}$  NMR (126 MHz, DMSO- $d_6$ )  $\delta$  172.3, 161.3, 159.5 (d,  $J$  = 3.0 Hz), 159.4, 148.9 (dd,  $J$  = 240.8, 4.8 Hz), 147.4 (t,  $J$  = 3.0 Hz), 140.6 (d,  $J$  = 8.8 Hz), 140.2 (d,  $J$  = 17.4

Hz), 138.8 (dd,  $J = 245.3$ , 6.6 Hz), 116.1, 110.6 (dd,  $J = 21.1$ , 2.9 Hz), 109.5 (d,  $J = 10.2$  Hz), 64.4, 63.0, 55.1, 40.1, 39.7, 38.1, 35.2, 28.2, 27.9, 25.2; HRMS (ESI<sup>-</sup>)  $m/z$  508.1471 (M - H<sup>+</sup>, C<sub>22</sub>H<sub>24</sub>F<sub>2</sub>N<sub>5</sub>O<sub>5</sub>S requires 508.1466).

**Methyl 5-((3*a*S,4*S*,6*a*R)-2-thioxohexahydro-1*H*-thieno[3,4-*d*]imidazol-4-yl)pentanoate (24).** D-Biotin methyl ester (387 mg, 1.50 mmol), prepared as previously reported,<sup>40</sup> was dissolved in xylenes (6 mL). Lawesson's reagent (607 mg, 1.50 mmol) was then added, and the reaction mixture was heated to 95 °C for 1 h. The solvent was removed under reduced pressure, and the resultant residue was extracted with ethyl acetate, dried, filtered, and evaporated under reduced pressure. The residue was purified using column chromatography over silica gel (eluent: CH<sub>2</sub>Cl<sub>2</sub>/CH<sub>3</sub>OH (50:1)) to afford **24** (330 mg, 80%) as a white solid. <sup>1</sup>H NMR (500 MHz, DMSO-*d*<sub>6</sub>) δ 8.24 (m, 1H), 8.17 (s, 1H), 4.54 (dd,  $J = 8.4$ , 5.0 Hz, 1H), 4.36 (ddd,  $J = 8.4$ , 4.5, 1.5 Hz, 1H), 3.58 (s, 3H), 3.17 (ddd,  $J = 8.6$ , 6.0, 4.5 Hz, 1H), 2.86 (dd,  $J = 12.6$ , 5.1 Hz, 1H), 2.67 (d,  $J = 12.7$  Hz, 1H), 2.30 (t,  $J = 7.5$  Hz, 2H), 1.77–1.24 (m, 6H); <sup>13</sup>C NMR (126 MHz, CDCl<sub>3</sub>) δ 182.4, 173.3, 66.0, 64.1, 55.7, 39.8, 33.1, 28.1, 27.9, 24.5; HRMS (ESI<sup>+</sup>)  $m/z$  297.0707 (M + Na<sup>+</sup>, C<sub>11</sub>H<sub>18</sub>N<sub>2</sub>O<sub>2</sub>S<sub>2</sub>Na requires 297.0707).

**5-((3*a*S,4*S*,6*a*R)-2-Thioxohexahydro-1*H*-thieno[3,4-*d*]imidazol-4-yl)pentanoic Acid (25).** To a solution of **24** (125 mg, 0.46 mmol) in CH<sub>3</sub>OH (4 mL) was added aq NaOH (1 N, 2 mL). The reaction mixture was heated to 35 °C for 0.5 h, followed by acidification with aq HCl (1 N, 10 mL). A precipitate formed, which was filtered, washed with cold aq HCl (1 N, 5 mL), and dried under high vacuum to give **25** (90 mg, 76%) as a white solid. <sup>1</sup>H NMR (500 MHz, DMSO-*d*<sub>6</sub>) δ 12.00 (s, 1H), 8.24 (s, 1H), 8.17 (s, 1H), 4.54 (dd,  $J = 8.4$ , 4.9 Hz, 1H), 4.36 (ddd,  $J = 8.5$ , 4.7, 1.4 Hz, 1H), 3.17 (ddd,  $J = 8.8$ , 5.9, 4.4 Hz, 1H), 2.86 (dd,  $J = 12.6$ , 5.0 Hz, 1H), 2.67 (d,  $J = 12.6$  Hz, 1H), 2.20 (t,  $J = 7.4$  Hz, 2H), 1.75–1.20 (m, 6H); <sup>13</sup>C NMR (126 MHz, DMSO-*d*<sub>6</sub>) δ 182.4, 174.5, 66.0, 64.1, 55.7, 40.1, 33.5, 28.2, 28.0, 24.6; HRMS (ESI<sup>-</sup>)  $m/z$  259.0572 (M - H<sup>+</sup>, C<sub>10</sub>H<sub>15</sub>N<sub>2</sub>O<sub>2</sub>S<sub>2</sub> requires 259.0575).

**6,8-Difluoro-7-hydroxy-2-oxo-N-(2-((3*a*S,4*S*,6*a*R)-2-thioxohexahydro-1*H*-thieno[3,4-*d*]imidazol-4-yl)pentanamido)ethyl)-2*H*-chromene-3-carboxamide (PB-Thiobiotin, 17).** Following the general procedure C, **25** (24 mg, 0.091 mmol) yielded compound **17** (18 mg, 49%) as a pale yellow solid. <sup>1</sup>H NMR (500 MHz, DMSO-*d*<sub>6</sub>) δ 8.79 (d,  $J = 1.4$  Hz, 1H), 8.66 (t,  $J = 5.8$  Hz, 1H), 8.23 (s, 1H), 8.15 (s, 1H), 7.92 (t,  $J = 5.6$  Hz, 1H), 7.73 (d,  $J = 10.5$  Hz, 1H), 4.69–4.46 (m, 1H), 4.34 (ddd,  $J = 8.5$ , 4.6, 1.6 Hz, 1H), 3.54–3.28 (m, 10H), 3.28–3.10 (m, 4H), 2.82 (dd,  $J = 12.7$ , 5.1 Hz, 1H), 2.65 (d,  $J = 12.7$  Hz, 1H), 2.15–1.97 (m, 2H), 1.74–1.16 (m, 6H); <sup>13</sup>C NMR (126 MHz, DMSO-*d*<sub>6</sub>) δ 182.4, 172.4, 161.5, 159.7, 149.3 (d,  $J = 239.7$  Hz), 147.4 (t,  $J = 2.8$  Hz), 140.8, 140.7, 139.0 (dd,  $J = 244.6$ , 6.8 Hz), 115.3, 110.6, 108.8, 66.0, 64.2, 55.8, 40.4, 40.1, 38.9, 35.3, 30.8, 28.3, 28.0, 25.3; HRMS (ESI<sup>-</sup>)  $m/z$  525.1050 (M - H<sup>+</sup>, C<sub>22</sub>H<sub>23</sub>F<sub>2</sub>N<sub>4</sub>O<sub>5</sub>S<sub>2</sub> requires 525.1078).

**Methyl 6-((4*R*,5*S*)-5-methyl-2-oxoimidazolidin-4-yl)-hexanoate (26).** To a solution of D-desthiobiotin (215 mg, 1.0 mmol) in CH<sub>3</sub>OH (5 mL), thionyl chloride (218 μL, 3.0 mmol) was added dropwise. The reaction mixture was stirred at 22 °C for 3 h. The solvent was removed under reduced pressure followed by purification using column chromatography on silica gel (eluent: CH<sub>2</sub>Cl<sub>2</sub>/CH<sub>3</sub>OH (20:1)) to afford **26** (217 mg, 95%) as a white solid. <sup>1</sup>H NMR (500 MHz, CDCl<sub>3</sub>) δ 5.34 (s, 1H), 5.07 (s, 1H), 3.89–3.78 (m, 1H), 3.70

(ddd,  $J = 9.2$ , 7.8, 4.9 Hz, 1H), 3.66 (s, 3H), 2.31 (t,  $J = 7.4$  Hz, 2H), 1.77–1.17 (m, 8H), 1.12 (d,  $J = 6.5$  Hz, 3H); <sup>13</sup>C NMR (126 MHz, CDCl<sub>3</sub>) δ 174.3, 164.0, 77.41, 77.36, 77.2, 76.9, 56.2, 51.7, 51.6, 34.0, 29.6, 29.1, 26.3, 24.8, 15.8; HRMS (ESI<sup>+</sup>)  $m/z$  251.1374 (M + H<sup>+</sup>, C<sub>11</sub>H<sub>20</sub>N<sub>2</sub>O<sub>3</sub>Na requires 251.1372).

**Methyl 6-((4*R*,5*S*)-5-methyl-2-thioxoimidazolidin-4-yl)-hexanoate (21).** To a solution of **26** (100 mg, 0.44 mmol) in xylenes (3 mL) was added Lawesson's reagent (178 mg, 0.44 mmol). The reaction mixture was heated to 95 °C for 1 h. The solvent was removed under reduced pressure, and the resultant residue was extracted with ethyl acetate, dried, filtered, and evaporated under reduced pressure. The residue was purified using column chromatography over silica gel (eluent: CH<sub>2</sub>Cl<sub>2</sub>/CH<sub>3</sub>OH (50:1)) to afford **21** (91 mg, 85%) as a white solid. <sup>1</sup>H NMR (500 MHz, CDCl<sub>3</sub>) δ 6.29 (br, 2H), 4.10 (t,  $J = 7.2$  Hz, 1H), 4.01–3.87 (m, 1H), 3.67 (s, 3H), 2.32 (t,  $J = 7.3$  Hz, 2H), 1.81–1.23 (m, 8H), 1.18 (d,  $J = 6.1$  Hz, 3H); <sup>13</sup>C NMR (126 MHz, CDCl<sub>3</sub>) δ 182.8, 174.1, 60.5, 55.9, 51.7, 34.0, 29.0, 28.9, 26.4, 24.8, 15.2; HRMS (ESI<sup>+</sup>)  $m/z$  267.1146 (M + Na<sup>+</sup>, C<sub>11</sub>H<sub>20</sub>N<sub>2</sub>O<sub>2</sub>SNa requires 267.1143).

**6-((4*R*,5*S*)-5-Methyl-2-thioxoimidazolidin-4-yl)hexanoic Acid (Imidazolidinethione, 20).** To a solution of **21** (63 mg, 0.26 mmol) in CH<sub>3</sub>OH (2 mL) was added aq NaOH (1 N, 1 mL). The reaction mixture was heated to 35 °C for 0.5 h followed by acidification with aq HCl (1 N, 5 mL). The resultant mixture was extracted with ethyl acetate, dried, filtered, and evaporated under reduced pressure. The residue was purified using column chromatography over silica gel (eluent: CH<sub>2</sub>Cl<sub>2</sub>/CH<sub>3</sub>OH (25:1)) to afford **20** (55 mg, 93%) as an off-white solid. <sup>1</sup>H NMR (500 MHz, CD<sub>3</sub>OD) δ 4.11–3.96 (m, 1H), 3.87 (dt,  $J = 8.8$ , 6.8 Hz, 1H), 2.30 (t,  $J = 7.4$  Hz, 2H), 1.71–1.25 (m, 8H), 1.13 (d,  $J = 6.6$  Hz, 3H); <sup>13</sup>C NMR (126 MHz, CD<sub>3</sub>OD) δ 183.5, 177.7, 61.4, 56.7, 34.8, 30.2, 30.0, 27.1, 25.9, 14.8; HRMS (ESI<sup>-</sup>)  $m/z$  229.1006 (M - H<sup>+</sup>, C<sub>10</sub>H<sub>17</sub>N<sub>2</sub>O<sub>2</sub>S requires 229.1011).

**6,8-Difluoro-7-hydroxy-N-(2-((4*R*,5*S*)-5-methyl-2-thioxoimidazolidin-4-yl)hexanamido)ethyl)-2-oxo-2*H*-chromene-3-carboxamide (PB-Imidazolidinethione, 18).** Following the general procedure C, **20** (23 mg, 0.1 mmol) yielded compound **18** (26 mg, 68%) as a pale yellow solid. <sup>1</sup>H NMR (500 MHz, DMSO-*d*<sub>6</sub>) δ 8.81 (br, 1H), 8.66 (t,  $J = 5.9$  Hz, 1H), 8.18 (s, 1H), 8.02 (s, 1H), 7.91 (t,  $J = 5.7$  Hz, 1H), 7.77 (dd,  $J = 10.6$ , 2.0 Hz, 1H), 3.92–3.77 (m, 1H), 3.68 (td,  $J = 8.2$ , 4.7 Hz, 1H), 3.37 (m, 2H), 3.21 (q,  $J = 6.1$  Hz, 2H), 2.05 (t,  $J = 7.4$  Hz, 2H), 1.58–1.08 (m, 8H), 0.96 (d,  $J = 6.4$  Hz, 3H); <sup>13</sup>C NMR (126 MHz, DMSO-*d*<sub>6</sub>) δ 181.8, 172.4, 161.3, 159.5, 148.9 (dd,  $J = 240.1$ , 4.1 Hz), 147.3 (d,  $J = 3.3$  Hz), 140.6 (d,  $J = 8.6$  Hz), 138.8 (dd,  $J = 245.1$ , 6.7 Hz), 116.1, 110.6 (dd,  $J = 21.6$ , 2.2 Hz), 109.4, 59.1, 54.4, 38.1, 35.4, 28.7, 28.6, 25.5, 25.2, 20.7, 14.6; HRMS (ESI<sup>-</sup>)  $m/z$  495.1534 (M - H<sup>+</sup>, C<sub>22</sub>H<sub>23</sub>F<sub>2</sub>N<sub>4</sub>O<sub>5</sub>S requires 495.1514).

**Benzyl 6-((5*S*)-5-methyl-2-oxoimidazolidin-4-yl)-hexanoate (27).** To a solution of D-desthiobiotin (100 mg, 0.46 mmol) in DMF (2 mL) was added benzyl alcohol (95 μL, 0.92 mmol), N-(3-dimethylaminopropyl)-N'-ethylcarbodiimide hydrochloride (EDC, 56 mg, 0.6 mmol), HOBt (92 mg, 0.6 mmol), and DMAP (56 mg, 0.46 mmol). The reaction mixture was stirred at 22 °C for 16 h. The solvent was removed under reduced pressure, and the residue was purified using column chromatography over silica gel (eluent: CH<sub>2</sub>Cl<sub>2</sub>/CH<sub>3</sub>OH (50:2)) to afford **27** (137 mg, 96%) as an off-white solid. <sup>1</sup>H NMR (500 MHz, CDCl<sub>3</sub>) δ 7.34–7.22 (m, 5H), 5.05 (s, 2H), 3.87–3.76 (m, 1H), 3.65 (td,  $J = 8.3$ , 5.0 Hz, 1H), 2.30 (t,  $J =$



7.4 Hz, 2H), 1.68–1.13 (m, 8H), 1.07 (d,  $J = 6.4$  Hz, 3H);  $^{13}\text{C}$  NMR (126 MHz,  $\text{CDCl}_3$ )  $\delta$  173.6, 163.4, 136.1, 128.7, 128.4, 66.3, 56.4, 51.8, 34.2, 29.5, 29.0, 26.3, 24.8, 15.8; HRMS (ESI+)  $m/z$  305.1889 ( $\text{M} + \text{H}^+$ ,  $\text{C}_{17}\text{H}_{24}\text{N}_2\text{O}_3$  requires 305.1865).

**Benzyl 6-((5S)-5-methyl-2-thioxoimidazolidin-4-yl)-hexanoate (Imidazolidinethione–OBn, 22).** To a solution of 27 (100 mg, 0.33 mmol) in xylenes (2.5 mL) was added Lawesson's reagent (133 mg, 0.33 mmol). The reaction mixture was heated to 95 °C for 1.5 h. The solvent was removed under reduced pressure, and the resultant residue was extracted with ethyl acetate, dried, filtered, and evaporated under reduced pressure. The residue was purified using column chromatography over silica gel (eluent:  $\text{CH}_2\text{Cl}_2/\text{CH}_3\text{OH}$  (50:1)) to afford 22 (86 mg, 82%) as an off-white solid.  $^1\text{H}$  NMR (500 MHz,  $\text{CDCl}_3$ )  $\delta$  7.45–7.27 (m, 5H), 5.11 (s, 2H), 4.07 (dq,  $J = 8.8$ , 6.5 Hz, 1H), 3.90 (td,  $J = 9.0$ , 4.8 Hz, 1H), 2.36 (t,  $J = 7.4$  Hz, 2H), 1.73–1.21 (m, 8H), 1.16 (d,  $J = 6.6$  Hz, 3H);  $^{13}\text{C}$  NMR (126 MHz,  $\text{CDCl}_3$ )  $\delta$  182.5, 173.4, 136.0, 128.6, 128.3, 66.2, 60.3, 55.8, 34.1, 28.8, 28.7, 26.2, 24.6, 15.0; HRMS (ESI+)  $m/z$  321.1652 ( $\text{M} + \text{H}^+$ ,  $\text{C}_{17}\text{H}_{24}\text{N}_2\text{O}_2\text{S}$  requires 321.1637).

**Assays of Binding of Small Molecules to SA.** SA protein from *Streptomyces avidinii* (lyophilized powder) was purchased from Alfa Aesar. Absorbance spectra and measurements of molar extinction coefficients ( $\epsilon$ ) were generated using semi-micro (1.4 mL) UV quartz cuvettes (Sigma-Aldrich, Z27667-7) on an Agilent 8452A diode array spectrometer. All optical spectroscopy and protein-binding assays were conducted in PBS (10 mM  $\text{Na}_2\text{HPO}_4$ , 137 mM NaCl, 2.7 mM KCl, and 1.8 mM  $\text{KH}_2\text{PO}_4$ , pH 7.4), unless otherwise noted. Molar extinction coefficients were determined in PBS (0.5% DMSO) and were calculated from Beer's Law plots of absorbance  $\lambda_{\text{max}}$  versus concentration, as shown in Figure S1. Linear least-squares fitting of the data (including a zero intercept) was used to determine the slope (corresponding to  $\epsilon$ ). Values ( $\text{M}^{-1} \text{cm}^{-1}$ ) were calculated as follows: absorbance =  $\epsilon[\text{concentration}(\text{M})]L$ , where  $L = 1$  cm. SA concentrations were quantified using UV absorbance at 280 nm based on its calculated molar extinction coefficient ( $\epsilon_{\text{monomer}} = 41\,326 \text{ M}^{-1} \text{cm}^{-1}$ ) using a Thermo Scientific NanoDrop 1000 spectrophotometer. All fluorescence spectra were acquired using a SUPRASIL ultra-micro quartz cuvette (PerkinElmer, B0631079) on a Perkin-Elmer LS55 fluorescence spectrometer (10 nm excitation and emission slit widths). Relative quantum yields ( $\Phi$ ) in PBS were determined by the Williams' method.<sup>41</sup> In brief, fluorophores were excited at 396 nm and the integrated fluorescence emission (415–700 nm) was quantified (concentrations of 5–160 nM). Coumarin 102 ( $\Phi = 0.66$  in water) provided the standard.<sup>42</sup> The integrated fluorescence emission at a given concentration was plotted against the maximum absorbance of the sample at that concentration, determined by extrapolation based on absorbance measurements at higher concentrations, as shown in Figure S1. Linear least-squares fitting of the data (including a zero intercept) was used to calculate the slope, which is proportional to the quantum yield. Quantum yields were calculated as follows:  $\Phi_x = \Phi_{\text{st}}(\text{Grad}_x/\text{Grad}_{\text{st}})$ , where  $\Phi_{\text{st}}$  represents the quantum yield of the standard,  $\Phi_x$  represents the quantum yield of the unknown, and Grad is the slope of the best linear fit. Theoretical Förster distances were calculated using a previously described protocol.<sup>43,44</sup> The following parameters and equations were used:  $\Phi_{\text{D}}$  is the quantum yield of the donor,  $\eta$  is the refractive index of the solvent,  $\kappa$  is the orientation factor,  $J$  is the degree of spectral overlap between the donor and the acceptor,

$F_{\text{D}}(\lambda)$  is the normalized donor fluorescence intensity, and  $\epsilon_{\text{A}}(\lambda)$  is the absorbance spectrum of the acceptor normalized to its maximum molar extinction coefficient.

$$R_0 = 0.0211[\kappa^2\phi_{\text{D}}\eta^{-4}J]^{1/6}$$

$$J = \int_{300}^{500} F_{\text{D}}(\lambda)\epsilon_{\text{A}}(\lambda)\lambda^4 d\lambda$$

Theoretical Förster distances were calculated using the PhotoChemCAD software, and the measured extinction coefficient for each probe were  $\Phi_{\text{tryptophan}} = 0.2$ ,  $\eta_{\text{phosphate buffer, pH 7.4}} = 1.33$ , and  $\kappa = 2/3$ .

**Determination of  $K_{\text{d}}$  Values Using FRET, Fluorescence Enhancement, and Fluorescence Quenching.** Different concentrations of SA protein, chosen to span a range of at least 20–80% complexation, were incubated with fixed concentrations of 16 (25 nM), 17 (5 nM), or 18 (25 nM) in PBS (pH 7.4) at room temperature with shaking for 1 h. These fixed probe concentrations were chosen to be substantially below the predicted  $K_{\text{d}}$  values to assure equilibrium binding measurements. Averages of three measurements of raw FRET values ( $I_{295}$ ,  $\lambda_{\text{ex}} = 295$  nm, and  $\lambda_{\text{em}} = 460$  nm) and fluorescence intensity values ( $I_{400}$ ,  $\lambda_{\text{ex}} = 400$  nm,  $\lambda_{\text{em}} = 460$  nm) were recorded for each sample using a Perkin-Elmer LS55 fluorescence spectrometer. These raw FRET values were corrected ( $I_{\text{ad}}$ ), and changes in fluorescence were corrected ( $I_{\text{ad},400}$ ) by subtracting background signals and factoring in quenching or enhancement of the fluorescence of PB upon binding as follows: averages of raw FRET ( $I_{\text{d},295}$ ) values and averages of the fluorescence ( $I_{\text{d},400}$ ) intensity of SA alone (background fluorescence) were calculated for each concentration of SA. Additionally, the average emission at 460 nm from three measurements of the free PB ligand (16–18 for direct binding and 18 for competition binding) in the PBS buffer upon excitation at 295 ( $I_{\text{a},295}$ ) and 400 nm ( $I_{\text{a},400}$ ) was calculated. Background-subtracted FRET ( $I_{\text{FRET}}$ ), fluorescence ( $I_{\text{ad},400}$ ), and the quenching ratio ( $Q_{\text{r}}$ ) were calculated as

$$I_{\text{FRET}} = I_{295} - I_{\text{a},295} - I_{\text{d},295}$$

$$I_{\text{ad},400} = I_{400} - I_{\text{d},400}$$

$$Q_{\text{r}} = \frac{I_{\text{ad},400}}{I_{\text{a},400}}$$

Background-subtracted FRET values ( $I_{\text{FRET}}$ ) were processed to directly factor in quenching or enhancement of fluorescence using the following equation, where  $I_{\text{ad}}$  is the corrected FRET signal

$$I_{\text{ad}} = \frac{I_{\text{FRET}}}{Q_{\text{r}}}$$

To calculate the dissociation constants ( $K_{\text{d}}$ ) using FRET (Figure 5), corrected FRET values ( $I_{\text{ad}}$ ), run in triplicate, were plotted against the concentration of SA (monomer) and a one-site-specific binding model (GraphPad Prism 6.0) was used for curve fitting.

To calculate the dissociation constants ( $K_{\text{d}}$ ) from simple enhancement or quenching of fluorescence (Figure 7), the change in fluorescence (enhancement or quenching,  $I_{\text{ad},400}$ ) was normalized and plotted against the concentration of SA (monomer). The experiments were run in triplicate, and a one-site-specific binding model (GraphPad Prism 6.0) was used

for curve fitting. For 17, the fluorescence intensity values for the three highest concentrations of the SA monomer (64, 128, and 256 nM) were excluded from the analysis to allow fitting of the one-site-specific binding model.

**Determination of  $K_i$  Values (Loss of Trp-FRET from Competitive Binding).** The unlabeled ligand was added to a fixed concentration of SA and fluorescent probe 18 (SA = 175 nM, 18 = 25 nM) in PBS (pH 7.4) precomplexed by incubation at room temperature with shaking for 1 h. The concentration of SA was chosen to be close to the  $K_d$  value measured for the fluorescent probe, and the concentration of 18 was chosen to be substantially below  $K_d$  to assure equilibrium binding. Measurements of raw FRET values ( $I_{295}$ ,  $\lambda_{ex} = 295$  nm,  $\lambda_{em} = 460$  nm) and fluorescence intensity values ( $I_{400}$ ,  $\lambda_{ex} = 400$  nm,  $\lambda_{em} = 460$  nm) were recorded for each sample using a Perkin-Elmer LS55 fluorescence spectrometer. Background subtraction and quenching were factored into each fluorescence measurement to calculate the corrected FRET signal ( $I_{ad}$ ) as described previously. To calculate  $IC_{50}$  values, the corrected FRET signal ( $I_{ad}$ ) was plotted against the concentration of the unlabeled ligand. The experiments were run in triplicate, and the log(inhibitor) versus response model (GraphPad Prism 6.0) was used for curve fitting. Inhibitory constants ( $K_i$ ) were calculated as

$$K_i = \frac{IC_{50}}{L/K_d + 1}$$

**ITC.** ITC experiments were performed using a MicroCal Auto-Isothermal Titration Calorimeter with protein and ligand solutions prepared in PBS. Titrations were performed at 25 °C and consisted of 25 injections (10  $\mu$ L) of the ligand (50–250  $\mu$ M) into SA (1.46 mL, 4–20  $\mu$ M), with 6 min between injections. The experimental data were fit to a one-site binding model (the Origin software), where  $\Delta H$  (enthalpy change, kcal/mol),  $K_a$  (association constant,  $M^{-1}$ ), and  $n$  (number of binding sites) were variables.

**Determination of  $K_d$  Values by FP of PB.** Fluorescence polarization is very sensitive to fluorescence quenching because of the effects on the lifetime of the fluorophore. This quenching prevented attempts to use FP to independently quantify the affinity of ligands 17 and 18 for SA.<sup>3</sup> However, quenching was less significant for the lower affinity ligand 16, and a previously described<sup>45</sup> FP method was used to independently analyze this probe. Measurements of fluorescence intensity ( $I_{400}$ ,  $\lambda_{ex} = 400$  nm,  $\lambda_{em} = 460$  nm) and fluorescence polarization ( $P$ ,  $\lambda_{ex} = 400$  nm,  $\lambda_{em} = 460$  nm) were recorded for each sample using a Perkin-Elmer LS55 fluorescence spectrometer. Background subtraction and quenching were factored into each fluorescence measurement to calculate the corrected fraction bound ( $f_a$ ), as described in the [Supporting Information](#). To calculate the dissociation constant ( $K_d$ ), the corrected fraction bound was plotted against the concentration of SA, and a one-site-specific binding model (GraphPad Prism 6.0) was used for curve fitting ([Figure S2](#)).

## ■ ASSOCIATED CONTENT

### ● Supporting Information

The Supporting Information is available free of charge on the ACS Publications website at DOI: [10.1021/acsomega.6b00356](https://doi.org/10.1021/acsomega.6b00356).

Additional experimental methods, data from binding assays and other photophysical measurements, and NMR spectra ([PDF](#))

## ■ AUTHOR INFORMATION

### Corresponding Author

\*E-mail: [brpeters@ku.edu](mailto:brpeters@ku.edu) (B.R.P.).

### ORCID

Blake R. Peterson: [0000-0001-8251-3579](https://orcid.org/0000-0001-8251-3579)

### Notes

The authors declare no competing financial interest.

## ■ ACKNOWLEDGMENTS

We thank the NIH (P20-GM103638 and P20-GM103418), the G. Harold and Leila Y. Mathers Charitable Foundation, and the KU Cancer Center for financial support. M.M.L. was supported in part by an NIH Dynamic Aspects of Chemical Biology training grant (T32-GM08545).

## ■ REFERENCES

- (1) Jelesarov, I.; Bosshard, H. R. Isothermal titration calorimetry and differential scanning calorimetry as complementary tools to investigate the energetics of biomolecular recognition. *J. Mol. Recognit.* **1999**, *12*, 3–18.
- (2) Pollard, T. D. A guide to simple and informative binding assays. *Mol. Biol. Cell* **2010**, *21*, 4061–4067.
- (3) Jameson, D. M.; Ross, J. A. Fluorescence polarization/anisotropy in diagnostics and imaging. *Chem. Rev.* **2010**, *110*, 2685–2708.
- (4) Wu, P. G.; Brand, L. Resonance energy transfer: Methods and applications. *Anal. Biochem.* **1994**, *218*, 1–13.
- (5) Zhang, H.; Wu, Q.; Berezin, M. Y. Fluorescence anisotropy (polarization): From drug screening to precision medicine. *Expert Opin. Drug Discov.* **2015**, *10*, 1145–1161.
- (6) Kim, J. H.; Sumranjit, J.; Kang, H. J.; Chung, S. J. Discovery of coumarin derivatives as fluorescence acceptors for intrinsic fluorescence resonance energy transfer of proteins. *Mol. Biosyst.* **2014**, *10*, 30–33.
- (7) Ghisaidoobe, A. B. T.; Chung, S. J. Intrinsic tryptophan fluorescence in the detection and analysis of proteins: A focus on Förster resonance energy transfer techniques. *Int. J. Mol. Sci.* **2014**, *15*, 22518–22538.
- (8) Zhang, Y.; Yang, X.; Liu, L.; Huang, Z.; Pu, J.; Long, G.; Zhang, L.; Liu, D.; Xu, B.; Liao, J.; Liao, F. Comparison of Förster-resonance-energy-transfer acceptors for tryptophan and tyrosine residues in native proteins as donors. *J. Fluoresc.* **2013**, *23*, 147–157.
- (9) Khazanov, N. A.; Carlson, H. A. Exploring the Composition of Protein–Ligand Binding Sites on a Large Scale. *PLoS Comput. Biol.* **2013**, *9*, No. e1003321.
- (10) Bogan, A. A.; Thorn, K. S. Anatomy of hot spots in protein interfaces. *J. Mol. Biol.* **1998**, *280*, 1–9.
- (11) Vivian, J. T.; Callis, P. R. Mechanisms of tryptophan fluorescence shifts in proteins. *Biophys. J.* **2001**, *80*, 2093–2109.
- (12) Chen, Y.; Barkley, M. D. Toward understanding tryptophan fluorescence in proteins. *Biochemistry* **1998**, *37*, 9976–9982.
- (13) Doody, M. C.; Gotto, A. M.; Smith, L. C. 5-(Dimethylamino)-naphthalene-1-sulfonic acid, a fluorescent probe of the medium chain fatty acid binding site of serum albumin. *Biochemistry* **1982**, *21*, 28–33.
- (14) Lakowicz, J. R.; Gryczynski, I.; Cheung, H. C.; Wang, C. K.; Johnson, M. L.; Joshi, N. Distance distributions in proteins recovered by using frequency-domain fluorometry. Applications to troponin I and its complex with troponin C. *Biochemistry* **1988**, *27*, 9149–9160.
- (15) Gustiananda, M.; Liggins, J. R.; Cummins, P. L.; Gready, J. E. Conformation of Prion Protein Repeat Peptides Probed by FRET Measurements and Molecular Dynamics Simulations. *Biophys. J.* **2004**, *86*, 2467–2483.
- (16) Fink, D. W.; Koehler, W. R. pH Effects on fluorescence of umbelliferone. *Anal. Chem.* **1970**, *42*, 990–993.
- (17) Sun, W.-C.; Gee, K. R.; Haugland, R. P. Synthesis of novel fluorinated coumarins: Excellent UV-light excitable fluorescent dyes. *Bioorg. Med. Chem. Lett.* **1998**, *8*, 3107–3110.

- (18) Chatterjee, A.; Maity, B.; Seth, D. Photophysics of 7-(diethylamino)coumarin-3-carboxylic acid in cationic micelles: Effect of chain length and head group of the surfactants and urea. *RSC Adv.* **2014**, *4*, 34026–34036.
- (19) Darbon, H.; Angelides, K. J. Structural mapping of the voltage-dependent sodium channel. Distance between the tetrodotoxin and Centruroides Suffusus Suffusus II beta-scorpion toxin receptors. *J. Biol. Chem.* **1984**, *259*, 6074–6084.
- (20) Liao, F.; Xie, Y.; Yang, X.; Deng, P.; Chen, Y.; Xie, G.; Zhu, S.; Liu, B.; Yuan, H.; Liao, J.; Zhao, Y.; Yu, M. Homogeneous noncompetitive assay of protein via Förster-resonance-energy-transfer with tryptophan residue(s) as intrinsic donor(s) and fluorescent ligand as acceptor. *Biosens. Bioelectron.* **2009**, *25*, 112–117.
- (21) Feng, Y.; Shen, X.; Chen, K.; Jiang, H.; Liu, D. A New Assay Based on Fluorescence Resonance Energy Transfer to Determine the Binding Affinity of Bcl-xL Inhibitors. *Biosci., Biotechnol., Biochem.* **2008**, *72*, 1936–1939.
- (22) Xie, Y.; Maxson, T.; Tor, Y. Fluorescent Ribonucleoside as a FRET Acceptor for Tryptophan in Native Proteins. *J. Am. Chem. Soc.* **2010**, *132*, 11896–11897.
- (23) Hang, J.; Shi, H.; Li, D.; Liao, Y.; Lian, D.; Xiao, Y.; Xue, H. Ligand binding and structural properties of segments of GABAA receptor alpha 1 subunit overexpressed in *Escherichia coli*. *J. Biol. Chem.* **2000**, *275*, 18818–18823.
- (24) Cohen, J. D.; Thompson, S.; Ting, A. Y. Structure-guided engineering of a Pacific Blue fluorophore ligase for specific protein imaging in living cells. *Biochemistry* **2011**, *50*, 8221–8225.
- (25) Chiesl, T. N.; Chu, W. K.; Stockton, A. M.; Amashukeli, X.; Grunthaler, F.; Mathies, R. A. Enhanced Amine and Amino Acid Analysis Using Pacific Blue and the Mars Organic Analyzer Microchip Capillary Electrophoresis System. *Anal. Chem.* **2009**, *81*, 2537–2544.
- (26) Kerkovius, J. K.; Menard, F. A Practical Synthesis of 6,8-Difluoro-7-hydroxycoumarin Derivatives for Fluorescence Applications. *Synthesis* **2016**, *48*, 1622–1629.
- (27) Green, N. M. In *Advances in Protein Chemistry*; Anfinsen, C. B., Frederic, J. J. T. E., Avidin, M. R., Eds.; Academic Press, 1975; Vol. 29, pp 85–133.
- (28) Le Trong, I.; Wang, Z.; Hyre, D. E.; Lybrand, T. P.; Stayton, P. S.; Stenkamp, R. E. Streptavidin and its biotin complex at atomic resolution. *Acta Crystallogr., Sect. D: Biol. Crystallogr.* **2011**, *D67*, 813–821.
- (29) Jones, M. L.; Kurzban, G. P. Noncooperativity of biotin binding to tetrameric streptavidin. *Biochemistry* **1995**, *34*, 11750–11756.
- (30) Chilkoti, A.; Tan, P. H.; Stayton, P. S. Site-directed mutagenesis studies of the high-affinity streptavidin-biotin complex: Contributions of tryptophan residues 79, 108, and 120. *Proc. Natl. Acad. Sci. U.S.A.* **1995**, *92*, 1754–1758.
- (31) Terai, T.; Kohno, M.; Boncompain, G.; Sugiyama, S.; Saito, N.; Fujikake, R.; Ueno, T.; Komatsu, T.; Hanaoka, K.; Okabe, T.; Urano, Y.; Perez, F.; Nagano, T. Artificial Ligands of Streptavidin (ALiS): Discovery, Characterization, and Application for Reversible Control of Intracellular Protein Transport. *J. Am. Chem. Soc.* **2015**, *137*, 10464–10467.
- (32) Xie, Y.; Yang, X.; Pu, J.; Zhao, Y.; Zhang, Y.; Xie, G.; Zheng, J.; Yuan, H.; Liao, F. Homogeneous competitive assay of ligand affinities based on quenching fluorescence of tyrosine/tryptophan residues in a protein via Förster-resonance-energy-transfer. *Spectrochim. Acta, Part A* **2010**, *77*, 869–876.
- (33) Trott, O.; Olson, A. J. AutoDock Vina: Improving the speed and accuracy of docking with a new scoring function, efficient optimization, and multithreading. *J. Comput. Chem.* **2010**, *31*, 455–461.
- (34) Nudelman, A.; Marcovici-Mizrahi, D.; Nudelman, A.; Flint, D.; Wittenbach, V. Inhibitors of biotin biosynthesis as potential herbicides. *Tetrahedron* **2004**, *60*, 1731–1748.
- (35) Green, N. M. Thermodynamics of the binding of biotin and some analogues by avidin. *Biochem. J.* **1966**, *101*, 774–780.
- (36) Raphael, M. P.; Rappole, C. A.; Kurihara, L. K.; Christodoulides, J. A.; Qadri, S. N.; Byers, J. M. Iminobiotin binding induces large fluorescent enhancements in avidin and streptavidin fluorescent conjugates and exhibits diverging pH-dependent binding affinities. *J. Fluoresc.* **2011**, *21*, 647–652.
- (37) Melkko, S.; Dumelin, C. E.; Scheuermann, J.; Neri, D. On the magnitude of the chelate effect for the recognition of proteins by pharmacophores scaffolded by self-assembling oligonucleotides. *Chem. Biol.* **2006**, *13*, 225–231.
- (38) Zhuang, Y.-D.; Chiang, P.-Y.; Wang, C.-W.; Tan, K.-T. Environment-sensitive fluorescent turn-on probes targeting hydrophobic ligand-binding domains for selective protein detection. *Angew. Chem., Int. Ed.* **2013**, *52*, 8124–8128.
- (39) Lee, M. J.; Pal, K.; Tasaki, T.; Roy, S.; Jiang, Y.; An, J. Y.; Banerjee, R.; Kwon, Y. T. Synthetic heterovalent inhibitors targeting recognition E3 components of the N-end rule pathway. *Proc. Natl. Acad. Sci. U.S.A.* **2008**, *105*, 100–105.
- (40) Chen, S.; Zhao, X.; Chen, J.; Chen, J.; Kuznetsova, L.; Wong, S. S.; Ojima, I. Mechanism-Based Tumor-Targeting Drug Delivery System. Validation of Efficient Vitamin Receptor-Mediated Endocytosis and Drug Release. *Bioconjug. Chem.* **2010**, *21*, 979–987.
- (41) Williams, A. T. R.; Winfield, S. A.; Miller, J. N. Relative Fluorescence Quantum Yields Using a Computer-Controlled Luminescence Spectrometer. *Analyst* **1983**, *108*, 1067–1071.
- (42) Jones, G.; Jackson, W. R.; Choi, C. Y.; Bergmark, W. R. Solvent effects on emission yield and lifetime for coumarin laser dyes. Requirements for a rotatory decay mechanism. *J. Phys. Chem.* **1985**, *89*, 294–300.
- (43) Hink, M. A.; Visser, N. V.; Borst, J. W.; van Hoek, A.; Visser, A. J. W. G. Practical Use of Corrected Fluorescence Excitation and Emission Spectra of Fluorescent Proteins in Förster Resonance Energy Transfer (FRET) Studies. *J. Fluoresc.* **2003**, *13*, 185–188.
- (44) Visser, A. J. W. G.; Vysotski, E. S.; Lee, J. Critical transfer distance determination between FRET pairs. **2011**, <http://www.photobiology.info/Experiments/Biolum-Expt.html>.
- (45) Jing, M.; Bowser, M. T. Methods for measuring aptamer-protein equilibria: A review. *Anal. Chim. Acta* **2011**, *686*, 9–18.